Identification of a High Affinity FcγRIIA-binding Peptide That Distinguishes FcγRIIA from FcγRIIB and Exploits FcγRIIA-mediated Phagocytosis and Degradation*□S

Gøril Berntzen[‡§1], Jan Terje Andersen[‡§], Kristine Ustgård[‡§], Terje E. Michaelsen[¶‖], Seyed Ali Mousavi[‡], Julie Dee Qian[‡§], Per Eugen Kristiansen[‡], Vigdis Lauvrak[‡2], and Inger Sandlie[‡§3]

From the ‡Department of Molecular Biosciences, University of Oslo, the §Centre for Immune Regulation, the ¶Norwegian Institute of Public Health, and the ‖Institute of Pharmacy, University of Oslo, Oslo, Norway

FcγRIIA is a key activating receptor linking immune complex formation with cellular effector functions. FcγRIIA has 93% identity with an inhibitory receptor, FcγRIIB, which negatively regulates FcγRIIA. FcγRIIA is important in the therapeutic action of several monoclonal antibodies. Binding molecules that discriminate FcγRIIA from FcγRIIB may optimize receptor activity and serve as a lead for development of therapeutics with FcγRIIA as a key target. Here we report the use of phage display libraries to select short peptides with distinct FcγRIIA binding properties. An 11-mer peptide (WAWVWLTETAV) was characterized that bound FcγRIIA with a K_d of 500 nM. It mediated cell internalization and degradation of a model antigen. The peptide-binding site on FcγRIIA was shown to involve Phe[163] and the IgG binding amino acids Trp[90] and Trp[113]. It is thus overlapping but not identical to that of IgG. Neither activating receptors FcγRI and FcγRIII, nor FcγRIIB, all of which lack Phe[163], bound the peptide.

Leukocyte IgG receptors (FcγRs) play a crucial role in immune protection by providing a link between antibody-antigen complexes and cellular effector functions. Two general classes of FcγRs are recognized: in humans they are the activating FcγRs I, IIA, and IIIA and the inhibitory FcγR IIB. The activating FcγRs are characterized by an intracellular tyrosine-based activation motif (ITAM),[4] which triggers an activating signaling cascade leading to phagocytosis, endocytosis, antibody-dependent cell cytotoxicity, and release of inflammatory mediators (1–3). By contrast, the inhibitory FcγRIIB contains an intracellular tyrosine-based inhibitory motif. Co-ligation of FcγRIIB with ITAM-containing receptors results in inhibition of ITAM-mediated functions (4–6). The balance of activation and inhibition through FcγRs is important for the regulation of immune function, setting thresholds for and ultimately determining the magnitude of the response.

FcγRIIA is the most widely expressed FcγR that is present on subgroups of leukocytes such as neutrophiles and mononuclear phagocytes, where the receptor exists in two common allelic forms at amino acid 134. The FcγRIIA-H134 allelotype (histidine) has higher binding efficiency for human IgG2 and IgG3 antibodies when compared with FcγRIIA-R131 (arginine) (7). The inhibitory FcγRIIB is expressed on the same cell types as FcγRIIA. In addition, FcγRIIB is expressed by B-cells, where this receptor is the only Fc receptor expressed.

Several studies have recognized that FcγRIIA is of particular importance in the anti-tumor activity of therapeutic monoclonal antibodies. FcγRIIA on leukocytes from patients undergoing granulocyte colony-stimulating factor treatment known to up-regulate FcγRIIA expression was shown to be the major trigger molecule for antibody-dependent cell cytotoxicity induced by an anti-HER-2/neu-specific IgG when various breast cancer cell lines were target cells in vitro (8). Furthermore, a study by Weng and Levy (9) showed a positive association of response rates in rituximab-treated non-Hodgkin's lymphoma patients with FcγRIIA-H134. Similarly, Zhang et al. (10) observed that metastatic colorectal cancer patients treated with an anti-epidermal growth factor receptor monoclonal antibody showed an FcγRIIA-R134-dependent progression-free survival. Taken together, these studies clearly demonstrate that FcγRIIA-dependent anti-tumor effects mediated by mononuclear phagocytes and/or neutrophils have considerable impact. Furthermore, FcγRIIA has a predominant role in infectious diseases (11, 12), and enhanced phagocytosis by this receptor may have a broad application in antibacterial therapy.

Although all FcγRs bind IgG immune complexes, individual FcγRs bind with affinities that vary depending on the IgG subclass involved (13). A high activating/inhibitory FcγR binding ratio was found to correlate with biological activity in models of tumor clearance and platelet depletion (14). In accordance with this, blocking FcγRIIB in mice resulted in enhanced tumor

□S The on-line version of this article (available at http://www.jbc.org) contains supplemental text, Tables S1–S4, and Figs. S1–S6.

[1] To whom correspondence may be addressed: Dept. of Molecular Biosciences, University of Oslo, P.O. Box 1041, 0316 Oslo, Norway. Tel.: 47-22-85-46-34; Fax: 47-22-85-60-41; E-mail: goril.berntzen@imbv.uio.no.
[2] Present address: Norwegian Knowledge Center for the Health Service, Olso, Norway.
[3] To whom correspondence may be addressed: Dept. of Molecular Biosciences, University of Oslo, P.O. Box 1041, 0316 Oslo, Norway. Tel.: 47-22-85-45-68; Fax: 47-22-85-60-41; E-mail: inger.sandlie@imbv.uio.no.

[4] The abbreviations used are: ITAM, intracellular tyrosine-based activation motif; GST, glutathione S-transferase; ELISA, enzyme-linked immunosorbent assay; PBS, phosphate-buffered saline; TU, transducing unit; FITC, fluorescein isothiocyanate; PMN, polymorphonuclear leukocyte; RU, resonance units; skm, skimmed milk.

immunity (15). Whereas FcγRIIIA-expressing NK cells implicated in antitumor antibody-dependent cell cytotoxicity (16) have been shown to infiltrate solid tumors poorly (17), the FcγRIIA/IIB-expressing cells (macrophages, DCs, neutrophils) do this very efficiently (18). Therefore, in such cases, selective engagement of FcγRIIA might be very efficacious, also because of the essential role of FcγRIIA in promoting uptake and presentation of antigens to both CD4^{+} (19) and CD8^{+} T-cells (20).

Because the extracellular domains of FcγRIIA and FcγRIIB are closely related in structure, having 93% amino acid identity in their extracellular domains, it has been challenging to design modified IgGs with mutations in the Fc region that distinguish between the two receptors (21). Strategies have been utilized to identify smaller molecules that target Fcγ receptors, including design of IgG-derived peptide sequences that mimic the part of IgG-Fc that binds Fcγ receptors (22–25), but still neither of these discriminates between the two receptors.

In the present study we performed selection from randomized phage display libraries to identify short novel peptides with distinct FcγRIIA binding properties. We identified, compared, and characterized several binders, and a phage displaying an 11-mer peptide (NNK11-C1) was characterized as the best binder. Binding of the NNK11-C1 phage was competed with free synthetic peptide with the same amino acid sequence, demonstrating that the peptide alone was sufficient for binding. The free peptide bound similarly to both allelic variants (Arg[134] and His[134]) with a K_d of 500 nM, whereas only very weak binding to FcγRIIB and no binding to FcγRI and FcγRIIIB was observed. The peptide was further shown to interfere with IgG binding. Comparing a panel of FcγRIIA and FcγRIIB mutants for their ability to bind the peptide, this was found to depend on the presence of Trp[90] and Trp[113] in addition to the proximal Phe[163] in FcγRIIA. Notably, whereas FcγRI, FcγRIIB, and FcγRIII harbor both Trp[90] and Trp[113], amino acid 163 is a valine in FcγRIII and a tyrosine in FcγRI and FcγRIIB. Thus, the presence of an aromatic, hydrophobic amino acid in position 163 was found to be the key to the actual binding specificity. Biotinylated peptide complexed on streptavidin-bound FcγRIIA on PMN and monocytes and mediated internalization and degradation of streptavidin coupled to 1 μM magnetic beads. This peptide may be an interesting candidate for development of therapeutics for optimal engagement of the immune system.

EXPERIMENTAL PROCEDURES

Cells and Antibodies—K562 (CCL-243) and 293E (CRL-10852) cells were purchased from the American Type Culture Collection (LGC Promochem, UK) and cultured as described (26). 293F cells were obtained from Invitrogen and cultured as described by the manufacturer. Leukocytes were drawn from peripheral blood from normal human volunteers as detailed elsewhere (27). Chimeric human IgG3 (chIgG3) was isolated from J558L cell lines as previously described (28). Biotinylated human IgG (hIgG-biot) was obtained by biotin labeling of normal pooled IgG (Tetagam, Aventis Behring, PA). Heat aggregation of IgG was done by incubation at 63 °C for 10 min.

Soluble FcγRs—Recombinant soluble human FcγRI was obtained from R & D Systems, Inc. (Minneapolis, MN), whereas recombinant soluble human FcγRIIIB (29) was kindly

provided by P. D. Sun (NIAID, National Institutes of Health, Rockville, MD). The extracellular domains of FcγRIIA-R134, FcγRIIA-H134, and FcγRIIB as well as the mutants IIA W90A, IIA W113A, IIA F163Y, IIB K130Q, IIB S135L, IIB N138T, IIB Y163F, and IIB K130Q/S135L/N138T/Y163F (IIB 4mut) were cloned and expressed as soluble fusions to GST in 293E cells as described in the supplemental text. The IIA mutants were all in Arg[134]. In addition, FcγRIIA-R134 and FcγRIIB were cloned and expressed as fusions to a His[6] tag (Supplementary methods).

ELISA—The FcγRII-GST and FcγRII-His fusion proteins were investigated for binding to hIgG by ELISA essentially as described (26). Briefly, the FcγRII proteins were coated in MaxiSorp microtiter strips (Nunc, Denmark). hIgG-biot or hIgG was added to FcγRII-GST or FcγRII-His, respectively, and bound IgG was detected by streptavidin conjugated to alkaline phosphatase (Amersham Biosciences) (FcγRII-GST) or horseradish peroxidase-conjugated goat anti-human IgG (Sigma) (FcγRIIA-His).

Phage Display Peptide Libraries and Phage Clones—The vector fUSE5 (30), which supports phage fd protein III (pIII) peptide expression, was used for library constructions. Two such libraries, Cys6 and Cys9, that represent 2.2×10^7 and 5×10^7 different cysteine-flanked peptides of six or nine random amino acids, respectively, have been described (31). A library of 11 random amino acids (NNK11) and three motif libraries, Evo1, Evo2, and Evo3, were similarly constructed using the primer *NNK$_{11}$* for the NNK11 library and the primers *Evo1*, *Evo2*, and *Evo3* (supplemental Table S1) (all from DNA Technology, Risskov, Denmark) for the three evolution libraries. The number of different clones in each library was estimated based on the number of primary transformants with insert. Control phages were randomly chosen from the Cys6 and Cys9 libraries. The Cys6 phage clone C6-1, with peptide insert CLRSGLGC, has previously been described and is selected for binding to FcγRI (26).

Selection of FcγRIIA-binding Peptides—Three consecutive rounds of selection from the Cys6, NNK11, Cys9, as well the three evolution libraries were performed. For the first round, wells precoated with 100 μl of goat anti-GST polyclonal antibody (Amersham Biosciences) were blocked for 1 h at room temperature with 1% PBS/skm. Aliquots of 100 μl of FcγRIIA-R134-GST (10 μg/ml) were added and incubated for 1 h at room temperature, followed by three washes with PBS/T. A total of 2×10^{11} *Escherichia coli* K91K transducing units (TUs) from the libraries diluted in 400 μl of PBS/skm were added to a total of four wells. After incubation for 1 h at room temperature followed by 10 washes with PBS/T, bound phages were eluted with 400 μl of 0.1 M HCl-glycine (pH 2.2), and eluates were neutralized with 28 μl of 1.5 M Tris (pH 8.8). Eluted phages were rescued as *E. coli* K91K transfectants, titrated, and amplified as described (30). Phage supernatant of the amplified eluate (E1A) was prepared essentially as described (30). For the second round of selection, two wells of MaxiSorp strips (Nunc) were coated overnight at 4 °C with 100 μl of FcγRIIA-R134-GST (10 μg/ml), blocked for 1 h at room temperature with 1% PBS/skm, and washed three times with PBS/T. A portion of E1A corresponding to 2.5×10^9 TU in PBS/skm was added to the wells.

Identification of a High Affinity FcγRIIA-binding Peptide

After incubation for 1 h at room temperature followed by 10 washes with PBS/T, bound phages were eluted, neutralized, rescued, and amplified as before. A third round of selection was performed with an input of 5×10^8 TU of the amplified second eluate (E2A) followed by the same procedure as described for the second round. Phage supernatants from single TUs were prepared as described (30).

Characterization of Phages—Aliquots of 5 or 50 μl of phage supernatants from amplified eluates or individual clones in a total of 100 or 200 μl 1% PBS/skm were allowed to react with FcγRII-GST fusion proteins, GST or PBS/skm coated in microtiter wells for 1 h at room temperature. The phage recovery was determined as described above. The amino acid sequences of peptides displayed by selected phages were determined by DNA sequencing (GATC Biotech, Konstanz, Germany) of PCR products as previously described (31).

Synthetic Peptides—Synthetic peptides were in the form ADGAX_nGAAK-Bio (Alta Bioscience), where ADGA and GAA are flanking amino acids as found in the fUSE5 phage, K-Bio represents a biotinylated lysine residue, and X_n represents selected peptides CPWFQWPC (C6-D), WAWVWLTETAV (NNK11-C1), and CTLRLGVGVRC (C9-E11) as well as a control peptide CWTSGARWRLC (RB-14). Peptides flanked by cysteines (C6-D, C9-E11, and RB-14) were produced as cyclic peptides. The RB-14 sequence has previously been selected for binding to poly(Ig) receptor (32) and was used as negative control. The synthetic peptides were purified by high pressure liquid chromatography to more than 80% purity (Alta Bioscience). The peptides were dissolved to 10 mM in Me$_2$SO (Sigma) and kept at $-20\,°C$.

Competition Assays with a Free Synthetic NNK11-C1 Peptide—Portions of 40 μM or 400 μM synthetic NNK11-C1 peptide were added to aliquots of 10 μl of supernatant of the NNK11-C1, C6-D phage, or a control phage displaying the peptide CDIF-GRDC and incubated in wells coated with 5 μg/ml FcγRIIA-R134-GST at 1 h at room temperature. The phage recovery was determined as described above.

ELISA Assays with Biotinylated Peptides—ELISA assays with biotinylated peptides were performed essentially as the ELISA for detection of bound hIgG to FcγRIIs as described (26). Briefly, synthetic biotinylated peptides in PBS were added in wells coated with FcγRII-GSTs and bound peptide detected by streptavidin conjugated to alkaline phosphatase.

Surface Plasmon Resonance Analyses—The instrument used for the SPR analysis was BIAcore 3000 (BIAcore AB, Uppsala, Sweden). The running buffer for all of the experiments was BIA-certified HBS buffer (10 mM HEPES, pH 7.4, 150 mM NaCl, 3.4 mM EDTA, 0.005% Surfactant P20). chIgG3 was covalently immobilized to ~1000 RU on a CM5 chip (BIAcore AB) with the amine coupling procedure. Serial dilutions (0.078–4 μM) of FcγRIIA-R134-His and FcγRIIB-His were injected over the sensor chip at a flow rate of 10 μl/min, and the binding reactions were allowed to reach (near) equilibrium. K_D was derived by nonlinear regression analysis of plots of R_{eq} (the equilibrium binding response) *versus* the analyte (chIgG3) concentration. The NNK11-C1-biotin peptide was captured on an SA chip (BIAcore AB) as described by the manufacturer, to ~50–100 RU followed by injection of recombinant human FcγRI (2 μM),

FcγRIIA-R134-His (1 μM), FcγRIIB-His (1 and 2 μM), and FcγRIIIB (2 μM) or serial dilutions (0.078–4 μM) of FcγRIIA-R134-His and FcγRIIB-His at a flow rate of 70 μl/min at 25 or 37 °C. For competitive studies 0.5 μM FcγRIIA-R134-His or FcγRIIB-His were preincubated with the NNK11-C1 peptide (2 and 50 μM) or chIgG3 (1 and 2 μM) and injected over immobilized chIgG3 or NNK11-C1 peptide, respectively. For all sensorgrams the signal from an uncoated reference cell was subtracted. Data evaluation was performed using BIAevaluation 4.1 Software (BIAcore AB).

FcγRII Sequence Analysis—ClustalW was used for sequence alignment of the extracellular domains of human FcγRIIA and FcγRIIB. The NCBI nucleotide accession numbers are NM_021642 (human FcγRIIA) and NM_004001 (human FcγRIIB). The stereo ribbon representation of the FcγRIIA structure was designed using MOLMOL with the crystallographic data of the FcγRIIA (33) available on the Protein Data Bank site. The structure of FcγRIIA (33) was superimposed onto the structure of FcγRIIB (34).

Circular Dichroism—The CD sample was dissolved in water. Trifluoroethanol was titrated to the water solution of the peptide at concentrations from 0 to 50%, and the CD data were recorded. The concentration of peptide was determined by absorption measurements at 280 nm using a Shimadzu UV-instrument (Shimadzu Corperation, Kyoto, Japan) before and after CD measurements. CD spectra were recorded using a Jasco J-810 spectropolarimeter (Jasco International Co., Ltd., Tokyo, Japan) calibrated with D-camphor-10-sulfonate (Icatayama Chemical, Tokyo, Japan). All of the measurements were taken up using a quartz cuvette (Starna, Essex, UK) with a path length of 0.1 cm. The samples were scanned five times at 50 nm/min with a bandwidth of 0.5 nm and a response time of 1 s, over the wavelength range 190–260 nm. The data were averaged, and the spectrum of a sample-free control was subtracted. The α-helical content of the peptide was determined by application of the single point method using the mean residual ellipticity at 222 nm ($[\theta]_{222}$) and the equation: $f_H = 100\% \times [\theta]_{222}/(\times 40{,}000(1-2.5n))$, where f_H is the α-helical content in %, and n is the number of residues (35). Two repetitions of each measurement were done.

Flow Cytometry Analysis—The PMN and monocyte populations of prepared leukocytes were identified in the scatter diagram in the flow cytometer and also verified by staining with mouse IgM anti-FcγRIIIB-FITC (Immunotech, Quebec, Canada) as a specific marker for human PMN, and mouse IgM anti-CD14-FITC conjugated to FITC (Coulter, Fullerton, CA) as a specific marker for human monocytes. Mouse IgM-FITC (Coulter) was used as negative isotype control. The binding of synthetic NNK11-C1-biotin (final concentration, 4 μM) was either detected by preformed complexes with streptavidin-FITC (Dako, Denmark) or with streptavidin-R-phycoerythrin (Dako). Fluorescence and scatter properties of cells were analyzed in Partec Cyto-Flow ML (Munster, Germany) flow cytometer.

Receptor-mediated Internalization and Degradation—Peptide-mediated internalization and degradation of streptavidin coupled to 1 μM magnetic beads (Invitrogen) were investigated essentially as described (26). Briefly, ^{125}I-labeled streptavidin-coupled magnetic beads were charged with the NNK11-C1

TABLE 1

Sequences of selected FcγRIIA-binding peptides from the Cys6 library

Sequence	Name/frequency
CAWYQFPC[a]	C6-A (6)[b]
CAWYEWPC	C6-B (12)
CVWWQWPC	C6-C (1)
CPWFQWPC	C6-D (1)
CKWFQWPC	C6-E (7)
CFWVNTDC	C6-F (1)
CLYLSIRC	C6-G (1)

[a] The consensus motif is showed in bold type.
[b] The number of clones with the peptide insert is shown in parentheses.

peptide and incubated with K562 cells, in the presence or absence of 0.6 μM concanamycin A (Sigma) or a combination of 1.6 μM leupeptin (Roche Applied Science) and 80 μM E64d (Calbiochem, Germany). Samples of supernatants were collected after 0, 3, and 6 h of incubation. Following precipitation with 10% trichloroacetic acid, acid-insoluble material, which represents cell-degraded ^{125}I-labeled streptavidin, was counted.

RESULTS

Production of Recombinant FcγRII-GST Fusion Proteins— The extracellular domains of FcγRIIA-R134, FcγRIIA-H134, and FcγRIIB were produced as recombinant GST fusion proteins as described in the supplemental text. All were purified on GST column and analyzed by SDS-PAGE electrophoresis where they appeared as bands of expected size (55 kDa) (not shown). Furthermore, all three variants bound heat-aggregated hIgG, the FcγRIIA variants slightly better than FcγRIIB (26), which is in agreement with data for FcγRs produced by others (36, 37).

Affinity Selection of FcγRIIA-binding Peptides from a Cys6 Library—Initially, a phage library of six random amino acids flanked by cysteines (the Cys6 library) was searched for binders to FcγRIIA-R134-GST as described under "Experimental Procedures." After three rounds of selection resulting in increasing output titer, individual clones were sequenced. Among 29 selected clones, seven different amino acid sequences were found (Table 1) five of which shared the consensus motif XW(F/Y/W)(Q/E)(W/F)P. They revealed up to 10 times increased recovery from wells coated with FcγRIIA-R134-GST compared with wells coated with skm or GST only (results not shown), and clone C6-D (CPWFQWPC) showed the highest recovery (Fig. 1*a*). Neither an FcγRI-binding phage clone, C6-1 (Fig. 1*a*) nor unselected phage clones (not shown) bound the target. Furthermore, the C6-D phage clone bound better to wells coated with FcγRIIA-R134-GST than to wells coated with FcγRIIB-GST (Fig. 1*b*).

In Vitro Evolution and Selections of New FcγRIIA Peptide Binders—To improve affinity by increasing the putative contact surface area between peptide and target, three evolution libraries based on the C6-D sequence were prepared. In the Evo1 library, the C6-D sequence was extended by three random amino acids (X) on each side (XXXCPWFQWPCXXX). In the Evo2 and Evo3 libraries, one proline and one of the flanking cysteines were excluded from the C6-D motif, and six random amino acids added to either side ($XXXXXX$WFQWPC and CPWFQW$XXXXXX$). In addition, a phage library of 11 random
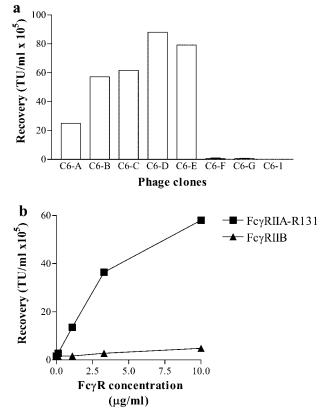
FIGURE 1. **Binding characteristics of individual phage clones from the Cys6 library after three rounds of selection on FcγRIIA-R134-GST.** Recovery of phage supernatants of ~2.5 × 10^8 TUs of the C6-A, C6-B, C6-C, C6-D, C6-E, C6-F, C6-G, and C6-1 clones after reaction with wells coated with 10 μg/ml FcγRIIA-R134-GST fusion protein (*a*) or of the C6D clone after reaction with wells coated with increasing concentrations (0–10 μg/ml) of FcγRIIA-R134-GST or FcγRIIB-GST (*b*).

amino acids (NNK11) was prepared as described under "Experimental Procedures." The sizes of the evolution libraries and the NNK11 library were estimated to be 1–3 × 10^7 and 9 × 10^8 different clones, respectively. DNA sequencing revealed the presence of diverse inserts of expected length (not shown). Three rounds of selection were performed as described under "Experimental Procedures," and selection from the three evolution libraries was compared with selection from the NNK11 library and also a Cys9 library of nine random amino acids flanked by cysteines, previously described (31) (supplemental Table S2).

Characterization of Individual Phage Clones—To characterize individual phage clones, supernatants from 10 to 30 individual isolates after three rounds of selection from each library were sequenced. The sequences are presented in Table 2, and an analysis of the sequences is included in the supplemental text. The clones were then screened for binding to FcγRIIA-R134-GST, and the clones with the best binding capacity from each library were then compared for binding to FcγRIIA-R134-GST, FcγR-H134-GST, FcγRIIB-GST, GST, and 1% skm. The results are summarized in Fig. 2. The NNK11-C1 clone showed thousand times increased recovery from wells coated with FcγRIIA-R134-GST as compared with the C6-D clone. In contrast, recovery from FcγRIIB-GST was 10-fold lower than that of the C6-D clone, as was background binding to skm. The

TABLE 2

Sequences of selected FcγRIIA-binding peptides from the Evo (1–3), Cys9, and NNK11 libraries

Library		Sequences of individual clones	
Evo1: XXXCPWFQWPCXXX	G2	VMKCPWFQWPCDAL	
	E2	VGGCPWFQWPCKGQ	(2)[a]
	E3	DQECPWFQWPCGAA	(2)
	E4	TRVCPWFQWPCVTG	(2)
	E7	RVRCPWFQWPCGMH	
	E10	SRSCPWFQWPCGSV	
	E12	TPNCPWFQWPCLKS	
Evo2: XXXXXXWFQWPC	B2	TDRMCRWFQWPC	
	D7	NSRDCAWFQWPC	
	A1	GEDRCLWFQWPC	
	D1	NKDECRWFQWPC	
	E1	IDSRCHWFQWPC	
	F1	GGMKCWWFQWPC	
	G1	GCNACAWFQWPC	
Evo3: CPWFQWXXXXXX	G10	CPWFQWPCLSHA	(2)
	G12	CPWFQWPCGARV	(2)
	G3	CPWFQWMLGCV	
	H9	CPWFQWSDSGCS	(4)
NNK11: XX	C1	WAWVVLTETAV	(23)
	B7	AVTFKFTGTDL	(2)
	C2	GSSHASLRYPA	
	C3	LLSFAGRSPSC	
	C7	LSGRSSGWRFS	
	D1	RLRFVVHESSG	
	D6	CPLGLLIHTSC	
Cys9: CC	A8	CCSVRGSAWAC	(2)
	A6	CILTIHGPLQC	(2)
	A5	CGARLAMAVAC	
	A2	CRDCVVACLGC	
	A1	CSMGLGGTSLC	
	A14	CGAPNLSRLLGC	
	E1	CGLGYRTAHIC	
	E11	CTLRLGVGVRC	
	E5	CHPHFPWATSC	

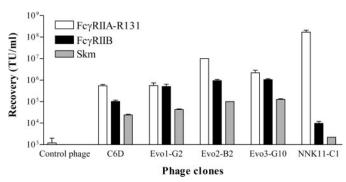[a] The number of clones with the peptide insert is shown in parentheses.

FIGURE 2. **Binding characteristics of the best binding phage clones from each of the Cys6, Cys9, NNK11, and Evo libraries after selection on FcγRIIA-R134-GST.** Recovery of phage supernatants of 5×10^8 to 1×10^9 TUs of the C6-D, NNK11-C1, Evo1-G2, Evo2-B3, and Evo3-G10 phage clones as well as an unselected control phage after reaction with wells coated with FcγRIIA-R134-GST (10 μg/ml), FcγRIIB-GST (10 μg/ml), or skm (1%).

clones selected from the evolution libraries (Evo1-G2, Evo2-B2 and Evo3-G10) showed up to 10-fold increased binding to both FcγRIIA-R134-GST and FcγRIIB-GST compared with the C6-D clone. However, these clones also revealed increased background binding to wells coated with 1% skm. None of the clones selected from the 9-mer library reached the binding capacity toward FcγRIIA-R134-GST as the C6-D clone (not shown). All of the clones tested showed equal binding to FcγRIIA-R134-GST and FcγRIIA-H134-GST (not shown).

Inhibition of the NNK11-C1 and C6-D Phage Binding to FcγRIIA by Free Peptide—Competition assays with a free synthetic peptide with NNK11-C1 sequence including the flanking residues ADGA and GAA from the phage format and a C-ter-
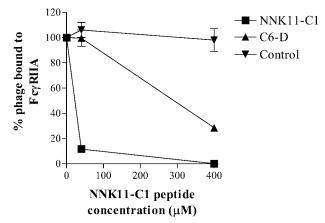

FIGURE 3. **Competition assays with a synthetic NNK11-C1 peptide (ADGAWAWVWLTETAVGAAK-Bio).** ELISA plates coated with FcγRIIA-R134-GST were incubated with free synthetic NNK11-C1 peptide (40 and 400 μM) for 1 h before the addition of NNK11-C1, C6-D, or control phages (1×10^9 TUs). Bound phages were detected as described under "Experimental Procedures" and expressed as a percentage of binding observed in the absence of competitor. The irrelevant peptide RB14 (ADGACWTSGARWRLGAAK-Bio) was used as control. The means of triplicates are shown.

minal Lys for conjugation of a biotin molecule (ADGAWAWVWLTETAVGAAK-Bio) showed clear inhibition of corresponding phage binding to FcγRIIA-R134-GST in ELISA (Fig. 3). Thus, the binding of the NNK11-C1 peptide to FcγRIIA was sequence-specific and not dependent on fusion to the phage. Furthermore, the peptide inhibited C6-D phage binding, although to a lesser extent. This suggests proximity of the binding sites for the two sequences on the receptor target. No inhibition of a control phage was observed.

Binding of Synthetic Peptides to FcγRIIA and FcγRIIB—Synthetic biotinylated variants of NNK11-C1 (as described above), C6-D (ADGACPWFQWPCGAAK-Bio), C9-E11 (ADGACTL-RLGVGVRCGAAK-Bio), and RB14 (as described above) were added to wells coated with FcγRIIA-R134-GST, FcγRIIA-H134-GST, and FcγRIIB-GST. NNK11-C1 bound the two allelic variants equally well (Fig. 4a), whereas ~200-fold more peptide was needed to give an A_{405} signal of ~0.9 for the NNK11-C1 binding to FcγRIIB (Fig. 4b). No binding above background was found for the remaining three peptides C6-D, C9-E11, and RB-14 at concentrations up to 100 μM (data not shown). In conclusion, the NNK11-C1 peptide binds equally well to both allelic variants of FcγRIIA but far less to FcγRIIB.

SPR Analysis of NNK11-C1 Peptide Binding to FcγRs and NNK11-C1 Peptide-mediated Inhibition of IgG Binding to FcγRIIA—The kinetics of the interaction between the synthetic NNK11-C1 peptide and FcγRIIs were studied using SPR. To circumvent potential aggregation of the GST-tagged receptor proteins (38, 39), FcγRIIA-R134-His and FcγRIIB-His were expressed as described in the supplemental text, and monomeric fractions of the receptors were isolated by size exclusion chromatography (supplemental Fig. S1). Both FcγRIIA-R134-His and FcγRIIB-His bound chIgG3 immobilized on a CM5 chip, and the steady state levels of the SPR responses (supplemental Fig. S2) were used to calculate the equilibrium affinity constants to be 1 and 2 μM (supplemental Table S3), respectively, which agrees with previous kinetic studies (37).
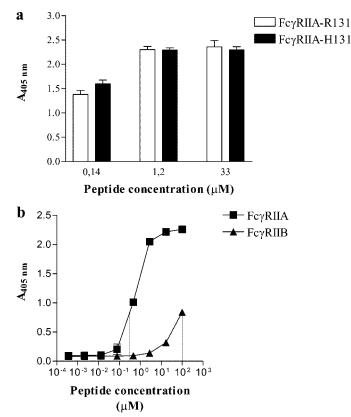
FIGURE 4. **Binding of synthetic peptides to FcγRIIA-R134-GST, FcγRIIA-H134-GST, and FcγRIIB-GST.** Various concentrations of synthetic biotinylated NNK11-C1 peptide was incubated in wells coated with FcγRIIA-R134-GST and FcγRIIA-H134-GST (*a*) or FcγRIIA-R134 and FcγRIIB-GST (*b*) (all at 0.09 μM). Bound peptide was detected with streptavidin conjugated to alkaline phosphatase. The *thin lines* indicate the peptide concentrations needed to give an A_{405} signal of 0.9. The data are expressed as A_{405} and represent the means of triplicates.

The synthetic biotinylated peptide was then immobilized on a SA chip, and samples of FcγRI (2 μM), FcγRIIA-R134-His (1 μM), FcγRIIB-His (1 and 2 μM), and FcγRIIIB (2 μM) were injected. The steady state level of the SPR response curve for the binding of FcγRIIA was set to 1. The data obtained showed increased binding of FcγRIIA compared with FcγRIIB, whereas binding of neither FcγRI nor FcγRIIIB was detected (Fig. 5*a*). Then serial injections of increasing concentrations (0.078–4 μM) of FcγRIIA-R134-His (supplemental Fig. S3) and FcγRIIB-His (data not shown) were injected. The kinetic rate constants (supplemental Table S4) were obtained using a heterogeneous ligand model, which gave the best global fit using the BIAevaluation 4.1 software. The model assumes that there are two independent parallel reactions with the immobilized NNK11-C1 peptide, which was determined to be at 0.5 μM (KD1) and 0.2 μM (KD2) at both 25 °C as well as 37 °C. This fitted well with the equilibrium-derived affinity constant of 0.5 μM (supplemental Table S4). The binding responses for the interaction between FcγRIIB-His and the NNK11-C1 peptide was too low for an affinity to be determined.

Injections of FcγRIIA-R134-His preincubated with an excess amount of chIgG3 over immobilized peptide resulted in decreased binding responses (Fig. 5*b*). The same was observed when FcγRIIA-His was preincubated with an excess amount of
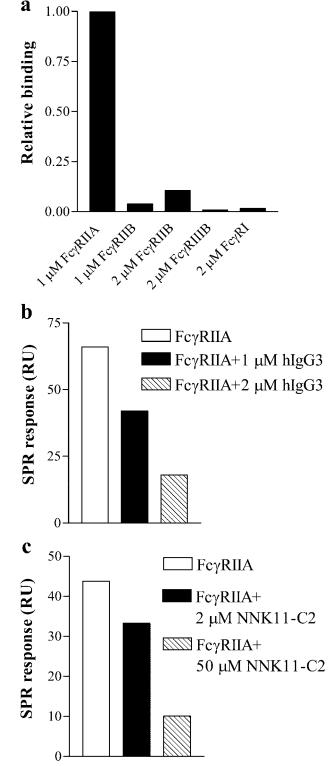

FIGURE 5. **SPR analysis of the interaction between synthetic NNK11-C1 peptide and FcγRI, FcγRIIA-R134-His, FcγRIIB-His, and FcγRIIIB.** *a*, synthetic biotinylated NNK11-C1 peptide was immobilized on an SA chip (~50–100 RU). Recombinant FcγRI (2 μM), FcγRIIA-R134-His (1 μM), FcγRIIB-His (1 and 2 μM), and FcγRIIIB (2 μM) were injected as described under "Experimental Procedures." The RU response near the steady state level of the interaction between FcγRIIA-R134-His and the immobilized peptide was set to 1, and relative SPR responses for the receptors were calculated. *b*, FcγRIIA-His (0.5 μM) injected in the absence or presence of chIgG3 (1 or 2 μM) over immobilized NNK11-C1 peptide (~50–100 RU). *c*, FcγRIIA-His (0.5 μM) injected in absence or presence of the NNK11-C1 peptide (2 or 5 μM) over immobilized hIgG1 (~1000 RU).

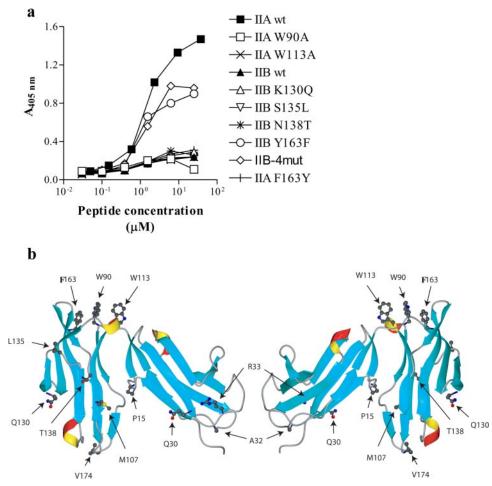# Identification of a High Affinity FcγRIIA-binding Peptide

FIGURE 6. **Binding of synthetic NNK11-C1 peptide to FcγRIIA and FcγRIIB mutants and stereo ribbon representation of the FcγRIIA structure.** *a*, various concentrations of synthetic biotinylated NNK11-C1 peptide was incubated in wells coated with FcγRIIA-R134-GST (*IIA wt*), FcγRIIB-GST (*IIB wt*), and the mutants indicated, all at 0.09 μM. Bound peptide was detected with streptavidin conjugated to alkaline phosphatase. The data are expressed as A_{405}. Similar data were obtained in three independent experiments. *b*, the residues that differ between FcγRIIA and FcγRIIB are indicated; Pro[15], Gln[30], Ala[32], Arg[33], Met[107], Gln[130], Leu[135], Thr[138], Phe[163], and Val[174]. Trp[90] and Trp[113] are involved in the IgG interacting site. The two drawings are oriented 180 ° to each other. The figure was designed using MOLMOL with the crystallographic data of FcγRIIA (33).

free peptide prior to injection over immobilized hIgG3 (Fig. 5*c*). Thus, the NNK11-C1 peptide interferes with hIgG3 binding to FcγRIIA.

Characterization of the Peptide-binding Site—To characterize the binding specificity of the peptide at the amino acid level, a number of FcγRIIA and FcγRIIB mutants were generated, coated in wells, and tested for peptide binding as before. First, the lack of NNK11-C1 binding to two FcγRIIA mutants, namely IIA W90A and IIA W113A, clearly demonstrated that both of these residues are critical for binding (Fig. 6*a*). Subsequently, the amino acid sequences of FcγRIIA and FcγRIIB were aligned (supplemental Fig. S4), and 10 residues found to differ between their extracellular parts, namely P15Q, Q30R, A32T, R33H, M107V, Q130K, L135S, T138N, F163Y, and V174A (Fig. 6*b*). Six are found in the cleft between the two Ig domains opposite the IgG interaction region involving Trp[90] and Trp[113]. Four (Gln[130], Leu[135], Thr[138], and Phe[163] in FcγRIIA) are, however, close to the IgG interaction surface in the folded molecule. Each and all four (IIB 4mut) were made FcγRIIA like on an FcγRIIB background, making a total of five FcγRIIB mutants. All were

coated as before and compared with wild type FcγRIIA and FcγRIIB for peptide binding. Interestingly, of the four amino acids tested, only one had a clear effect, namely IIB Y163F. Both IIB Y163F and IIB 4mut showed increased peptide binding compared with FcγRIIB wild type and the other three mutants. An FcγRIIA mutant where F163 was made IIB-like (IIA F163Y) lost peptide binding ability (Fig. 6*a*). Thus, a single hydroxyl group is at the core of the IIA/IIB discrimination shown by the selected peptide.

CD Analysis of the NNK11-C1 Peptide—The NNK11-C1 peptide precipitated fast from water as well as methanol and ethanol solutions. In spite of this, we were able to obtain CD spectra of the peptide in water. In addition, the CD spectra in water:trifluoroethanol was obtained (supplemental Fig. S5). NNK11-C1 did not have a well defined structure in water but formed an α-helix in mixtures of water and trifluoroethanol, with an α-helical content of 54% in 50% trifluoroethanol solution.

Flow Cytometry Analysis of NNK11-C1 Peptide Binding to PMN and Monocytes—Biotinylated peptide was complexed to streptavidin-FITC as described under "Experimental Procedures" and incubated with peripheral blood leukocytes before analyzes by flow cytometry. The scatter diagrams were gated for PMN, monocytes, and lymphocytes. Both PMN and monocytes bound the NNK11-C1 peptide, whereas no binding to the irrelevant control peptide RB14 was seen (Fig. 7). The phenotype of the gated PMN and monocyte preparations was verified by staining with anti-FcγRIIIB-FITC (PMN) and anti-CD14-FITC (monocytes), respectively (data not shown). In contrast, when gating on the lymphocyte fraction, no binding of NNK11-C1 was observed (Fig. 7). Again, this demonstrates the FcγRIIA specificity of the peptide, as normal B-cells express FcγRIIB because their only Fc receptor and the B-cells in the lymphocyte population were negative. Aggregated hIgG showed a dose-dependent inhibition of binding of NNK11-C1 peptide complexed to streptavidin (supplemental Fig. S6), which again suggested overlapping binding sites.

The NNK11-C1 Peptide Induces Receptor-mediated Internalization—The functional properties of the NNK11-C1 peptide as regarding induction of FcγRIIA-mediated internalization and degradation was demonstrated as follows. Aggregates of the NNK11-C1 peptide were prepared by incubation of bio-
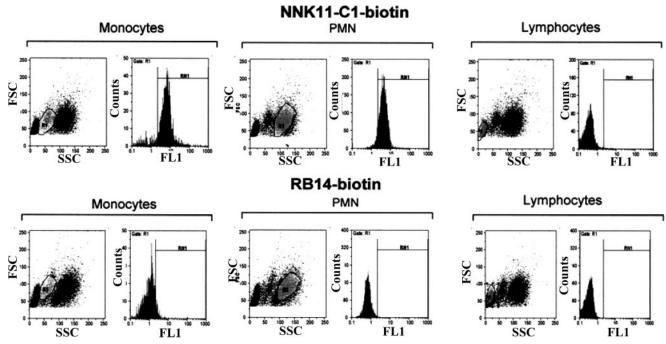
NNK11-C1-biotin

RB14-biotin

FIGURE 7. **Flow cytometry analysis of NNK11-C1 peptide binding to human peripheral blood PMN, monocytes and lymphocytes.** Freshly prepared leukocytes were incubated with preformed complexes of NNK11-C1-biotin or RB14-biotin (both at 4 μM) and streptavidin-FITC. The regions were set on monocytes (*left panel*), PMNs (*middle panel*), and lymphocytes (*right panel*) and analyzed for binding.
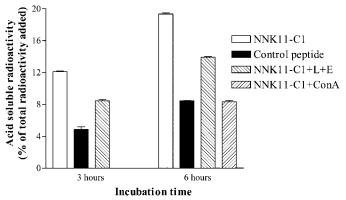

FIGURE 8. **Study of NNK11-C1-mediated cell internalization and vesicular degradation.** K562 cells were incubated with ^{125}I-strep-beads-NNK11-C1 with and without the addition of 0.6 μM concanamycin A (*ConA*) or a combination of 80 μM E64d (*E*) and 1.6 mM leupeptin (*L*). After 3 and 6 h, release of acid-soluble radioactivity into the medium was measured. ^{125}I-strep-beads-RB14 was included as control. Concanamycin A was added to the 6-h samples only. The data represent the means of two representative experiments.

tinylated NNK11-C1 peptide with iodinated (^{125}I) streptavidin on 1-μm magnetic beads. The beads were then incubated with K562 cells at 37 °C for 3 or 6 h, and the degradation of streptavidin was estimated as previously described (26). The cells that were stimulated with beads loaded with the NNK11-C1 peptide degraded significantly more streptavidin than cells incubated with beads loaded with the irrelevant control peptide (RB14), at both time points (Fig. 8). Both concanamycin A (inhibitor of the vacuolar proton pump) and a combination of E64d (inhibitor of lysosomal thiol proteases) and leupeptin (inhibitor of lysosomal serine and cysteine proteases) prevented the formation of acid-soluble cpm in the medium, suggesting that degradation of streptavidin took place in late acidic endocytic compartments (late endosomes/lysosomes).

DISCUSSION

Through a comprehensive selection strategy, we identified a peptide that bound specifically and with high affinity to the human activating FcγRIIA. The peptide, derived from an 11-mer library and denoted NNK11-C1, bound with similar affinity to both allelic variants of the receptor, FcγRIIA-H134 and FcγRIIA-R134, showed very low binding to the inhibitory FcγRIIB, and showed no binding to two other activating FcγRs, namely FcγRI and FcγRIIIB. Peptide binding to FcγRIIA competed with binding of the natural ligand, hIgG. Polymerized peptide mediated targeting of streptavidin to cells expressing FcγRIIA and promoted internalization and degradation of this model antigen in acid vesicles.

We used two different phage display based strategies to select specific peptide binders to FcγRIIA. In an "evolution approach" a core consensus motif of six amino acids was isolated, and the best binder identified (C6-D) was further extended with four or six flanking amino acids. In the second approach, two libraries of either 11 random amino acids or nine random amino acids constrained by cysteines were searched for binders. The C6-D phage clone distinguished somewhat between FcγRIIA and FcγRIIB. After sequence extension and additional rounds of selection, binding to FcγRIIA increased. However, so did binding to FcγRIIB and blocking reagent. In contrast to this, a single phage clone from the 11-mer library, NNK11-C1, had the desired binding characteristics with three logs better recovery from FcγRIIA than C6-D and four logs better recovery on FcγRIIA than on FcγRIIB. Also, free synthetic peptide bound FcγRIIA in ELISA and discriminated exceptionally well between FcγRIIA and FcγRIIB.

Furthermore, the same free synthetic peptide preparation inhibited binding of phages displaying either NNK11-1C or C6-D, and both strategies thus selected binders to overlapping

sites on the receptor. The fact that NNK11-1C was inhibited to a greater extent than C6-D and that NNK11-1C discriminates better than C6-D between FcγRIIA and FcγRIIB argues against the binding sites being identical. That the NNK11-C1 peptide binds at or close to the IgG-binding site was demonstrated in two independent SPR-based assays where FcγRIIA was preincubated with IgG and tested for binding to immobilized peptide, or vice versa, preincubated with peptide and tested for binding to immobilized IgG. In either case, less complexed than free receptor was bound. Also, the interference with the IgG-binding site was verified by flow cytometry analysis of NNK11-C1 binding to PMN and monocytes.

The specificity of the peptide was further confirmed by SPR measurements, which revealed binding to FcγRIIA at an affinity of 0.5 μM, greatly reduced binding to FcγRIIB and almost no binding to FcγRI and FcγRIIIB. The affinity toward FcγRIIA was slightly increased compared with hIgG, which is important for any future clinical application of the NNK11-C1 peptide.

The selected peptides all contain several aromatic amino acids and in particular tryptophane. It should be noted that a high number of aromatic amino acids is commonly found among phage display selected peptides (31, 40–42). Also in native proteins, aromatic amino acids play an important role in folding and recognition and are often found as part of binding sites for small ligands and enzyme substrates (43, 44). Other sequences with specificity for FcγRI that were previously selected from the same Cys6 library that was used in the present study did not contain tryptophanes (26). Thus, the selection of tryptophane depends on the nature of the target binding site and not the library *per se*. Interestingly, peptide FcγRIIA binders recently identified (45) also contain two tryptophane residues. The best binder, CWPGWDLNC (C7C1), selected from a 7-mer library, has striking similarities with C6-D described here. Mutagenesis within the C7C1 peptide showed that W2A and P3A lost affinity for FcγRIIA, and these amino acids are also present in C6-D. Binding of C7C1 was inhibited by IgG. Because NMR structure analyses of C7C1 revealed a type II β-turn between the two tryptophanes and solvent-exposed proline, a binding mode was suggested where the proline is inserted between Trp[90] and Trp[113] on FcγRIIA, mimicking the interaction between FcγRIIA and IgG (46, 47). The argument may hold for C6-D as well. Because Trp[90] and Trp[113] are found in both FcγRIIA and FcγRIIB, this would explain why the short C6-D peptide and the sequences derived from C6-D distinguish poorly between the two receptors. In contrast, the NNK11-C1 peptide showed a great increase in binding to FcγRIIA compared with FcγRIIB. Both W90A and W113A IIA mutants lost affinity for the peptide, demonstrating that binding is indeed dependent on Trp[90] and Trp[113], found on both receptors, and part of the IgG-binding site. Notably, the affinity of NNK11-C1 for FcγRIIA was measured to be 200 times better than the 100 μM found for C7C1. Because the NNK11-C1 peptide is longer than C7C1, it may offer the possibility for a greater interaction surface between the peptide and FcγRIIA. Mutational analysis revealed that Phe[163] in FcγRIIA is part of this interaction surface. Phe[163] is in very close proximity to the two tryptophanes in the folded molecule, and the peptide may bind the extended site whether it forms a β-sheet or has an α-helical conformation.
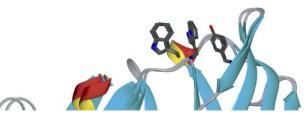

FIGURE 9. **The structure of FcγRIIA superimposed over the structure of FcγRIIB.** The structures show Trp[90] and Trp[113] central to the IgG-binding site, as well as the amino acid residue 163. The figure was designed using MOL-MOL with the crystallographic data of FcγRIIA (33) and FcγRIIB (34).

Residue 163 is a tyrosine in FcγRI and FcγRIIB and a valine in FcγRIIIA and FcγRIIIB, which indicates that the peptide has a requirement for an aromatic, hydrophobic amino acid in this position that allows for hydrophobic stacking. This particular amino acid is not a part of the IgG interaction site with FcγRIII (46, 47).

Both the FcγRIIB Y163F mutant and the FcγRIIB mutant where all amino acids at the IgG binding surface were IIA-like showed increased peptide binding. The level did, however, not quite reach that of FcγRIIA. Amino acids in the cleft between the two Ig domains may contribute. An overlay of FcγRIIA and FcγRIIB structures (Fig. 9) shows the two tryptophanes central to the IgG-binding site, as well as amino acid residue 163. Notably, the 163 Y/F transition alters neither the main chain nor the side chain position. The peptide thus seems to discriminate between the absence and presence of a single hydroxyl group.

Important features for usefulness in clinical settings of targeting peptides are high affinity to ligand, low immunogenicity, and absence of unwanted side effects. We believe that the ability of the short NNK11-C1 peptide sequence to exploit FcγRIIA-mediated uptake and degradation without interfering with the inhibitory FcγRIIB makes this ligand an interesting candidate for further studies. Furthermore, the ability of the NNK11-C1 peptide to bind to FcγRIIA in an allele-independent fashion suggests potential applications of this molecule in patients who carry the low binding allele.

REFERENCES

1. Daeron, M. (1997) *Annu. Rev. Immunol.* **15,** 203–234
2. Gessner, J. E., Heiken, H., Tamm, A., and Schmidt, R. E. (1998) *Ann. Hematol.* **76,** 231–248
3. Ravetch, J. V., and Bolland, S. (2001) *Annu. Rev. Immunol.* **19,** 275–290
4. Hunter, S., Indik, Z. K., Kim, M. K., Cauley, M. D., Park, J. G., and Schreiber, A. D. (1998) *Blood* **91,** 1762–1768
5. Van den Herik-Oudijk, I. E., Capel, P. J., van der Bruggen, T., and Van de Winkel, J. G. (1995) *Blood* **85,** 2202–2211
6. Daeron, M., Latour, S., Malbec, O., Espinosa, E., Pina, P., Pasmans, S., and Fridman, W. H. (1995) *Immunity* **3,** 635–646
7. Shields, R. L., Namenuk, A. K., Hong, K., Meng, Y. G., Rae, J., Briggs, J., Xie, D., Lai, J., Stadlen, A., Li, B., Fox, J. A., and Presta, L. G. (2001) *J. Biol. Chem.* **276,** 6591–6604
8. Stockmeyer, B., Valerius, T., Repp, R., Heijnen, I. A., Buhring, H. J., Deo, Y. M., Kalden, J. R., Gramatzki, M., and van de Winkel, J. G. (1997) *Cancer Res.* **57,** 696–701
9. Weng, W. K., and Levy, R. (2003) *J. Clin. Oncol.* **21,** 3940–3947
10. Zhang, W., Gordon, M., Schultheis, A. M., Yang, D. Y., Nagashima, F.,

Azuma, M., Chang, H. M., Borucka, E., Lurje, G., Sherrod, A. E., Iqbal, S., Groshen, S., and Lenz, H. J. (2007) *J. Clin. Oncol.* **25,** 3712–3718

11. Platonov, A. E., Shipulin, G. A., Vershinina, I. V., Dankert, J., van de Winkel, J. G., and Kuijper, E. J. (1998) *Clin. Infect. Dis.* **27,** 746–750

12. Yuan, F. F., Wong, M., Pererva, N., Keating, J., Davis, A. R., Bryant, J. A., and Sullivan, J. S. (2003) *Immunol. Cell Biol.* **81,** 192–195

13. Nimmerjahn, F., Bruhns, P., Horiuchi, K., and Ravetch, J. V. (2005) *Immunity* **23,** 41–51

14. Nimmerjahn, F., and Ravetch, J. V. (2005) *Science* **310,** 1510–1512

15. Kalergis, A. M., and Ravetch, J. V. (2002) *J. Exp. Med.* **195,** 1653–1659

16. Sulica, A., Morel, P., Metes, D., and Herberman, R. B. (2001) *Int. Rev. Immunol.* **20,** 371–414

17. Albertsson, P. A., Basse, P. H., Hokland, M., Goldfarb, R. H., Nagelkerke, J. F., Nannmark, U., and Kuppen, P. J. (2003) *Trends Immunol.* **24,** 603–609

18. Mantovani, A., Sozzani, S., Locati, M., Allavena, P., and Sica, A. (2002) *Trends Immunol.* **23,** 549–555

19. Benitez-Ribas, D., Adema, G. J., Winkels, G., Klasen, I. S., Punt, C. J., Figdor, C. G., and de Vries, I. J. (2006) *J. Exp. Med.* **203,** 1629–1635

20. Liu, Y., Gao, X., Masuda, E., Redecha, P. B., Blank, M. C., and Pricop, L. (2006) *J. Immunol.* **177,** 8440–8447

21. Armour, K. L., van de Winkel, J. G., Williamson, L. M., and Clark, M. R. (2003) *Mol. Immunol.* **40,** 585–593

22. Medgyesi, D., Uray, K., Sallai, K., Hudecz, F., Koncz, G., Abramson, J., Pecht, I., Sarmay, G., and Gergely, J. (2004) *Eur. J. Immunol.* **34,** 1127–1135

23. Radaev, S., and Sun, P. D. (2001) *J. Biol. Chem.* **276,** 16478–16483

24. Sheridan, J. M., Hayes, G. M., and Austen, B. M. (1999) *J. Pept. Sci.* **5,** 555–562

25. Uray, K., Medgyesi, D., Hilbert, A., Sarmay, G., Gergely, J., and Hudecz, F. (2004) *J. Mol. Recognit.* **17,** 95–105

26. Berntzen, G., Brekke, O. H., Mousavi, S. A., Andersen, J. T., Michaelsen, T. E., Berg, T., Sandlie, I., and Lauvrak, V. (2006) *Protein Eng. Des. Sel.* **19,** 121–128

27. Michaelsen, T. E., Ihle, O., Beckstrom, K. J., Herstad, T. K., Kolberg, J., Hoiby, E. A., and Aase, A. (2003) *Infect. Immun.* **71,** 5714–5723

28. Michaelsen, T. E., Garred, P., and Aase, A. (1991) *Eur. J. Immunol.* **21,** 11–16

29. Zhang, Y., Boesen, C. C., Radaev, S., Brooks, A. G., Fridman, W. H., Sautes-Fridman, C., and Sun, P. D. (2000) *Immunity* **13,** 387–395

30. Smith, G. P., and Scott, J. K. (1993) *Methods Enzymol.* **217,** 228–257

31. Lauvrak, V., Berntzen, G., Heggelund, U., Herstad, T. K., Sandin, R. H., Dalseg, R., Rosenqvist, E., Sandlie, I., and Michaelsen, T. E. (2004) *Scand. J. Immunol.* **59,** 373–384

32. Braathen, R., Sandvik, A., Berntzen, G., Hammerschmidt, S., Fleckenstein, B., Sandlie, I., Brandtzaeg, P., Johansen, F. E., and Lauvrak, V. (2006) *J. Biol. Chem.* **281,** 7075–7081

33. Maxwell, K. F., Powell, M. S., Hulett, M. D., Barton, P. A., McKenzie, I. F., Garrett, T. P., and Hogarth, P. M. (1999) *Nat. Struct. Biol.* **6,** 437–442

34. Sondermann, P., Huber, R., and Jacob, U. (1999) *EMBO J.* **18,** 1095–1103

35. Scholtz, J. M., Qian, H., York, E. J., Stewart, J. M., and Baldwin, R. L. (1991) *Biopolymers* **31,** 1463–1470

36. Sondermann, P., Jacob, U., Kutscher, C., and Frey, J. (1999) *Biochemistry* **38,** 8469–8477

37. Maenaka, K., van der Merwe, P. A., Stuart, D. I., Jones, E. Y., and Sondermann, P. (2001) *J. Biol. Chem.* **276,** 44898–44904

38. Kaplan, W., Husler, P., Klump, H., Erhardt, J., Sluis-Cremer, N., and Dirr, H. (1997) *Protein Sci.* **6,** 399–406

39. Tudyka, T., and Skerra, A. (1997) *Protein Sci.* **6,** 2180–2187

40. Xu, X., Wang, S., Hu, Y. X., and McKay, D. B. (2007) *J. Mol. Biol.* **373,** 367–381

41. Hsu, C. L., Chen, Y. L., Yeh, S., Ting, H. J., Hu, Y. C., Lin, H., Wang, X., and Chang, C. (2003) *J. Biol. Chem.* **278,** 23691–23698

42. Gebhardt, K., Lauvrak, V., Babaie, E., Eijsink, V., and Lindqvist, B. H. (1996) *Pept. Res.* **9,** 269–278

43. Burley, S. K., and Petsko, G. A. (1985) *Science* **229,** 23–28

44. Raine, A. R., Yang, C. C., Packman, L. C., White, S. A., Mathews, F. S., and Scrutton, N. S. (1995) *Protein Sci.* **4,** 2625–2628

45. Cendron, A. C., Wines, B. D., Brownlee, R. T., Ramsland, P. A., Pietersz, G. A., and Hogarth, P. M. (2008) *Mol. Immunol.* **45,** 307–319

46. Radaev, S., Motyka, S., Fridman, W. H., Sautes-Fridman, C., and Sun, P. D. (2001) *J. Biol. Chem.* **276,** 16469–16477

47. Sondermann, P., Huber, R., Oosthuizen, V., and Jacob, U. (2000) *Nature* **406,** 267–273

SUPPLEMENTAL METHODS

Cloning and production of GST- and (His)$_6$-tagged FcγRIIA/B variants - The extracellular domains of FcγRIIA-R134 and FcγRIIB were cloned and expressed as soluble fusions to GST in 293E cells as previously described[1] or in 293F cells as described by the manufacturer. The extracellular domains of the allotypic FcγRIIA-H134 variant was produced by a PCR splicing by overlap extension (PCR SOEing) technique with the mutagenic primers *R134H-1* and *R134H-2*, and the primers *FcγRIIA-forw* and *FcγRIIA-back* (Supplemental Table S1) (all from DNA Technology) using the vector pcDNA3(oriP)-FcγRIIA[1] as template. The mutants IIA W90A, IIA W113A, IIA F163Y, IIB K130Q, IIB S135L, IIB N138T, IIB Y163F and IIB K130Q-S135L-N138T-Y163F (IIB 4mut) were produced by QuickChange^{TM} site-directed mutagenesis (Stratagene) with the corresponding mutagenic primers listed in Supplemental Table S1 using the vectors pcDNA3(oriP)-FcγRIIA[1] and pcDNA3(oriP)-FcγRIIB[1], respectively, as templates. All PCR products were subcloned on HindIII-XhoI sites into the vector pcDNA3(oriP)-FcγRIIA or pcDNA3(oriP)-FcγRIIB, so as to replace FcγRIIA-R134 or FcγRIIB. All FcγRII-GST fusion proteins were purified as previously detailed[1]. The pcDNA3(oriP)-FcγRIIA and pcDNA3(oriP)-FcγRIIB vectors were further utilized as templates in PCR SOEing reactions to exchange the GST-tags with (His)$_6$-tags, using the primers *FcγRIIA-His-1* or *FcγRIIB-His-1* and *FcγRIIA/B-2* and the primers *pcDNA3-forw* and *pcDNA3-back* (Supplemental Table S1) (all from Eurogentech, Seraing, Belgium). The PCR-products were subcloned on HindIII-AvrII sites so as to replace the sequence encoding the GST-tag with the (His)$_6$ tag. The recombinant proteins, termed FcγRIIA-R134-His and FcγRIIB-His were purified using a HisTrap™ FF Ni Sepharose 6 Fast Flow column (Amersham Biosciences). Elution buffer was exchanged with PBS on Amicron Ultra–15 (Millipore, MA, USA), and monomeric fractions of FcγRIIA-R134-His and FcγRIIB-His were isolated on a Superdex 200 column (GE Healthcare, CT, USA), as described by the manufacturer. Protein concentration was determined by NanoDrop® ND-1000 Spectrophotometry (NanoDrop Technologies, Wilmington, DE, USA).

SDS-PAGE and western blotting - Portions of 3 μg or 100 ng of FcγRIIA-R134-His and FcγRIIB-His were separated by non-reducing 12% Bis/Tris XT Criterion precast gel (Bio-Rad, Hercules, CA USA). The gels (3 μg receptor protein) were either stained with Bio-Safe^{TM} Coomassie Brilliant Blue (Bio-Rad), or the proteins (100 ng) were blottet onto a polyvinylidene fluoride membrane (Millipore) in Tris-glycine buffer (25 mM Tris, 1092 mM glycine, and 20 % methanol, pH 8.3) at 25 V for 30 min using semi-dry blotting apparatus (Bio-Rad). The membrane was blocked in PBS/skm before receptors were detected with goat anti-CD32B MAb (1:5000; R&D Systems) followed by mouse anti-goat-HRP (1:5000; Sigma). The membrane was washed and developed with SuperSignal^{TM} West Pico substrate (Pierce, Rockford, IL, USA) and exposed to BioMax^{TM} MR film (Kodak, Fernwald, Germany).

SUPPLEMENTAL RESULTS

Analysis of sequences after three rounds of selection - More than two thirds of the isolates from the NNK11 library shared the sequence WAWVWLTETAV (NNK11-C1). Nine different sequences from the Cys9 library contained short stretches of similarity, but without a clear consensus motif. Six different sequences selected from the Evo1 library, revealed no obvious similarities in the region flanking the C6-D motif. Seven different sequences isolated from the Evo2 library all contained cysteine in the same position as in the Cys6 phages. Except for the

presence of charged amino acids, no obvious similarity was found among these clones. For the Evo3 library, four different sequences were found. Notably, two (Evo3-G12 and Evo3-G10) contained both the proline (P) and the cysteine (C) in the same position as the C6-D phage. The two others (Evo3-G3 and Evo3-H9) had a cysteine further down in the sequence. The sequences are presented in Table 2.

REFERENCES

1. Berntzen, G., Lunde E., Flobakk M., Andersen J., Lauvrak, V., and Sandlie, I. (2005) *J. Immunol. Methods* **298**, 93-104.

SUPPLEMENTAL FIGURE LEGENDS

SUPPLEMENTAL FIGURE S1. **Production of monomeric FcγRIIA-R134-His and FcγRIIB-His.** Receptor proteins were expressed as described in Methods. Monomeric fractions were isolated by size exclusion chromatography, and separated by (a) non-reducing SDS PAGE followed by (b) western blotting and receptor detection as described.

SUPPLEMENTAL FIGURE S2. **The resonance profile for the equilibrium binding between IgG3 and FcγRIIA-R134-His or FcγRIIB-His.** Increasing concentrations (0.078 - 4 µM) of soluble (a) FcγRIIA-R134-His or (b) FcγRIIB-His were injected over immobilized hIgG3 (~1000 RU). The steady state levels of the SPR responses were used to calculate the affinities.

SUPPLEMENTAL FIGURE S3. **The receonance profile for the interaction between synthetic NNK11-C1 peptide and FcγRIIA-R134-His.** Increasing concentrations (0.078 - 4 µM) of FcγRIIA-R134-His were injected over immobilized NNK11-C1 peptide (~50-100 RU). The kinetic rate values were calculated by fitting the binding data to a heterogeneous ligand model.

SUPPLEMENTAL FIGURE S4. **Sequence alignment of the extracellular domains of human FcγRIIA and FcγRIIB.** Amino acid residues that are identical in all sequences are indicated by (*), conserved substitutions are indicated by (:), and semi-conservative substitutions are indicated by (.).

SUPPLEMENTAL FIGURE S5. **CD spectra of the NNK11-C1 peptide.** The solid line shows the CD spectrum of the NNK11-C1 peptide in water while the dotted line shows the CD spectrum in water:TFE 1:1.

SUPPLEMENTAL FIGURE S6. **Freshly prepared leucocytes were preincubated with aggregated hIgG before addition of NNK11-C1/strep-FITC complexes.** The final concentration of NNK11-C1 was 4µM and the final inhibiting concentration of aggragated hIgG was 4 µM (1), 0.4 µM (2), 0.04 µM (3) and no hIgG (4).

SUPPLEMENTAL TABLES

SUPPLEMENTAL TABLE 1
Primer sequences

Primer	Sequence
R134H- 1	5'-GTC TTT AAG AGG **GTA**[1] AAC CTA GGG -3' reverser denne
R134H-2	5'-CAG AAA TTC TCC **CAT** TTG GAT CCC -3'
FcγRIIA-forw	5'-TA TAT AAG CTT ATG GCT ATG GAG ACC CAA ATG TCT CA-3'
FcγRIIA-back	5'-TA TAT AAG CTT ATG GCT ATG GAG ACC CAA ATG TCT CA-3'
FcγRIIA-W90A-forw	5'-CTT TCC GAA **GCG** CTG GTG CTC-3'
FcγRIIA-W90A-back	5'-GAG CAC CAG **CGC** TTC GGA AAG-3'
FcγRIIA-W113A-forw	5'-TGC CAC AGC **GCG** AAG GAC AAG-3'
FcγRIIA-W113A-back	5'-CTT GTC CTT **CGC** GCT GTG GCA-3'
FcγRIIB-K130Q-forw	5'-C GGA AAA TCC **CAG** AAA TTT TCC CG '3
FcγRIIB-K130Q-back	5'-CG GGA AAA TTT **CTG** GGA TTT TCC G '3
FcγRIIB-S135L-forw	5'-TTT TCC CGT **CTG** GAT CCC AAC-3'
FcγRIIB-S135L-back	5'-GTT GGG ATC **CAG** ACG GGA AAA-3'
FcγRIIB-N138T-forw	5'-TCG GAT CCC **ACC** TTC TCC ATC-3'
FcγRIIB-N138T-back	5'-GAT GGA GAA **GGT** GGG ATC CGA-3'
FcγRIIB-Y163F-forw	5'- TAC ACG CTG **TTC** TCA TCC AAG-3'
FcγRIIB-Y163F-back	5'-CTT GGA GTA **GAA** CAG CGT GTA-3'
FcγRIIA-F163Y-forw	5'-TAC ACG CTG **TAC** TCA TCC AAG-3'
FcγRIIA-F163Y-back	5'-CTT GGA TGA **GTA** CAG CGT GTA-3'
FcγRIIA-His-1	5'-TA TAT AAG CTT ATG GCT ATG GAG ACC CAA ATG TCT CA-3'

Fcγ RIIB-His-1	5'-TA TAT AAG CTT ATG GGA ATC CTG TCA TTT TTA CCT GTC C-3'
Fcγ RIIA/B-2	5'-TCA GTG ATG GTG ATG GTG ATG ACT ACC ACC-3'
pcDNA3-forw	5'-GGT GGT AGT CAT CAC CAT CAC CAT CAC TGA CCC GGG CCC TAT TCT ATA CTT GTA-3'
pcDNA3-back	5'-TAT ATA CCT AGG CCT CCA AAA AAG CCT CCT C-3'
NNK$_{11}$	5'-C TAT TCT CAC TCG GCC GAC GGG GCC (NNK^2)$_{11}$ GGG GCC GCT GGG GCC GAA ACT GTT GAA-3'
Evo1	5'-C TAT TCT CAC TCG GCC GAC GGG GCC (NNK)$_3$ TGT CCT TGG TTT CAG TGG CCG TGT (NNK)$_3$ GGG GCC GCT GGG GCC GAA ACT GTT GAA-3'
Evo2	5'-C TAT TCT CAC TCG GCC GAC GGG GCC (NNK)$_6$ TGG TTT CAG TGG CCG TGT GGG GCC GCT GGG GCC GAA ACT GTT GAA-3'
Evo3	5' C TAT TCT CAC TCG GCC GAC GGG GCC TGT CCT TGG TTT CAG TGG (NNK)$_6$ GGG GCC GCT GGG GCC GAA ACT GTT GAA-3'

[1]Mismatched nucleotides are shown in bold
[2]N: A,C,G or T; K: G or T

SUPPLEMENTAL TABLE S2
Selection from the Evo (1-3), Cys9 and NNK11 libraries; percentage recovery of third round eluates[1].

Library	FcγRIIA-R134-GST	GST	1% Skm
Evo1: XXXCPWFQWPCXXX	0.03 %	$6x10^{-4}$ %	$5x10^{-3}$ %
Evo2: XXXXXXWFQWPC	0.10 %	$6x10^{-4}$ %	$8x10^{-3}$ %
Evo3: CPWFQWXXXXXX	0.18 %	$2x10^{-3}$ %	$1x10^{-3}$ %
NNK11: XXXXXXXXXXX	0.8 %	$2x10^{-3}$ %	$6x10^{-4}$ %
Cys9: CXXXXXXXXXC	0.08 %	$6x10^{-5}$ %	$5x10^{-3}$ %

[1] Percentage recovery after addition of 2-3.5 x 10^7 TU of phage from the amplified third round eluates to wells coated with 10µg/ml FcγRIIA-R134-GST, 5µg/ml GST, or wells with blocking solution (1% skm). Recovery was determined as E.coli K91K TUs in acid eluates

SUPPLEMENTAL TABLE S3
Equilibrium constants for the interactions between hIgG3 and FcγRIIA/FcγRIIB

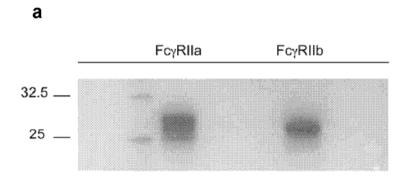| Analyte	Equilibrium KD[1] (µM)
CD32A	1.0 ± 0.1
CD32B	1.99 ± 0.04

[1] Due to fast kinetics the steady state binding levels were used to determined the equilibrium affinity constants from near equilibrium plots.
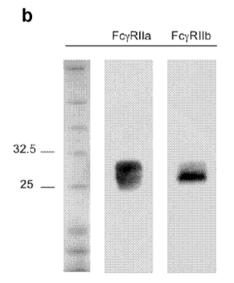
SUPPLEMENTAL TABLE S4
Surface plasmon resonance derived kinetic and equilibrium constants for the interactions between free synthetic NNK11-C1 peptide and FcγRIIA/FcγRIIB
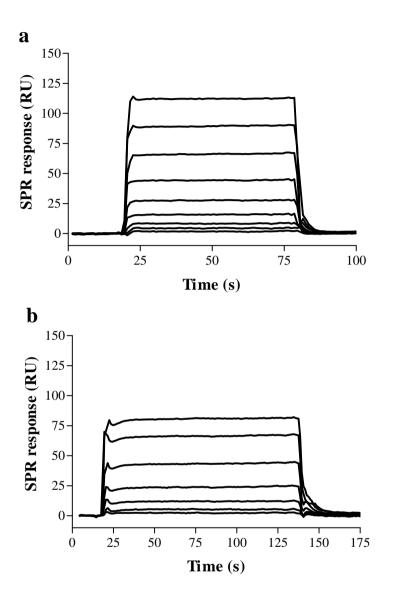
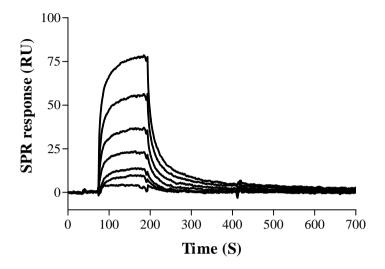| Analyte	ka1 (1/Ms)	kd1 (1/s)	ka2 (1/Ms)	kd2 (1/s)	KA1 (1/M)	KA2 (1/M)	Kd1 (μM)	Kd2 (μM)	Equ KD[1] (μM)
FcγRIIA[2]	1.2 e5 ±0.1e5	0.059 ±0.005	2.0 e4 ±0.2e4	3.7 e-3 ±0.2e-3	2.01e6 ±0.06e6	5.8 e6 ±0.1e6	0.50 ±0.02	0.19 ±0.03	0.53 ±0.002
FcγRIIA[3]	3.40e5 ±0.04 e5	0.17 ±0.01	3.2e4 ±0.1e4	7.6e-3 ±0.1e-3	2.0e6 ±0.1e6	4.24e6 ±0.03e6	0.50 ±0.05	0.235 ±0.002	-
FcγRIIB	ND[4]	ND	ND	ND	ND	ND	ND	ND	ND

[1] The equilibrium affinity constants were estimated from near equilibrium plots.

[2] The kinetic rate constants were obtained using a heterogeneous ligand model.

[3] The measurements were performed at 37°C instead of 25°C.

[4] Not determined (ND) due to no or very low detectable binding responses.
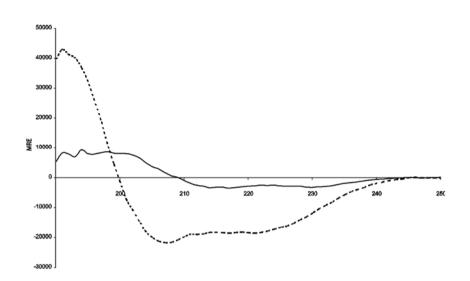
SUPPLEMENTAL FIGURE S1

a

FcγRIIa   FcγRIIb

32.5 ——

25 ——

Coomassie stain: 3μg protein

b

FcγRIIa   FcγRIIb

32.5 ——

25 ——

SUPPLEMENTAL FIGURE S2

SUPPLEMENTAL FIGURE S3
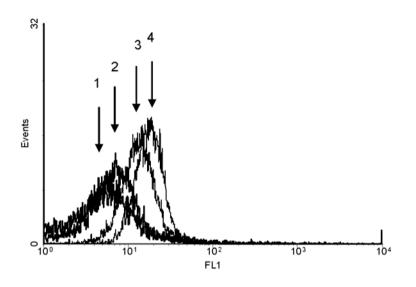
SUPPLEMENTAL FIGURE S4

```
FcγRIIA      3 AAPPKAVLKLEPPWINVLQEDSVTLTCQGARSPESDSIQWFHNGNLIPTHTQPSYRFKANNNDSGEYTCQTGQTSL  78
FcγRIIB      3 AAPPKAVLKLEPQWINVLQEDSVTLTCRGTHSPESDSIQWFHNGNLIPTHTQPSYRFKANNNDSGEYTCQTGQTSL  78
               ************ **************:*.:*********************************************

FcγRIIA     79 SDPVHLTVLSEWLVLQTPHLEFQEGETIMLRCHSWKDKPLVKVTFFQNGKSQKFSRLDPTFSIPQANHSHSGDYHC 154
FcγRIIB     79 SDPVHLTVLSEWLVLQTPHLEFQEGETIVLRCHSWKDKPLVKVTFFQNGKSKKFSRSDPNFSIPQANHSHSGDYHC 154
               ***************************:***********************:**** **.***************

FcγRIIA    155 TGNIGYTLFSSKPVTITVQVPSMGSSSPM 184
FcγRIIB    155 TGNIGYTLYSSKPVTITVQAP---SSSPM 184
               ********:**********.*   *****
```

SUPPLEMENTAL FIGURE S5

SUPPLEMENTAL FIGURE S6

Identification of a High Affinity FcγRIIA-binding Peptide That Distinguishes Fcγ RIIA from FcγRIIB and Exploits FcγRIIA-mediated Phagocytosis and Degradation

Gøril Berntzen, Jan Terje Andersen, Kristine Ustgård, Terje E. Michaelsen, Seyed Ali Mousavi, Julie Dee Qian, Per Eugen Kristiansen, Vigdis Lauvrak and Inger Sandlie

Access the most updated version of this article at doi: 10.1074/jbc.M803584200

Alerts:
- When this article is cited
- When a correction for this article is posted

Click here to choose from all of JBC's e-mail alerts

Supplemental material:
http://www.jbc.org/content/suppl/2008/10/29/M803584200.DC1

This article cites 47 references, 20 of which can be accessed free at
http://www.jbc.org/content/284/2/1126.full.html#ref-list-1